Published in final edited form as:
Adv Funct Mater. 2010 September 23; 20(18): 3154–3162. doi:10.1002/adfm.201000390.

Thickness Dependent Properties of Relaxor-$PbTiO_3$ Ferroelectrics for Ultrasonic Transducers

Hyeong Jae Lee,
Materials Research Institute, Department of Materials Science & Engineering, The Pennsylvania State University, University Park, PA, 16802 (USA)

Shujun Zhang[*] **[Prof.]**,
Materials Research Institute, Department of Materials Science & Engineering, The Pennsylvania State University, University Park, PA, 16802 (USA)

Dr. Jun Luo,
TRS Technologies, Inc., 2820 East College Avenue, State College, PA 16801 (USA)

Fei Li, and
Materials Research Institute, Department of Materials Science & Engineering, The Pennsylvania State University, University Park, PA, 16802 (USA)

Thomas R. Shrout
Materials Research Institute, Department of Materials Science & Engineering, The Pennsylvania State University, University Park, PA, 16802 (USA)

Abstract

The electrical properties of $Pb(Mg_{1/3}Nb_{2/3})O_3$-$PbTiO_3$ (PMN-PT) based polycrystalline ceramics and single crystals were investigated as a function of scale ranging from 500 microns to 30 microns. Fine-grained PMN-PT ceramics exhibited comparable dielectric and piezoelectric properties to their coarse-grained counterpart in the low frequency range (<10 MHz), but offered greater mechanical strength and improved property stability with decreasing thickness, corresponding to higher operating frequencies (>40 MHz). For PMN-PT single crystals, however, the dielectric and electromechanical properties degraded with decreasing thickness, while ternary $Pb(In_{1/2}Nb_{1/2})O_3$-$Pb(Mg_{1/3}Nb_{2/3})O_3$-$PbTiO_3$ (PIN-PMN-PT) exhibited minimal size dependent behavior. The origin of property degradation of PMN-PT crystals was further studied by investigating the dielectric permittivity at high temperatures, and domain observations using optical polarized light microscopy. The results demonstrated that the thickness dependent properties of relaxor-PT ferroelectrics are closely related to the domain size with respect to the associated macroscopic scale of the samples.

Keywords

Structure-Property Relationships; Dielectric; Ferroics; Relaxor-PT

1. Introduction

Ultrasound imaging is the most widely used imaging technique in the field of medical diagnosis. The increase in operational frequency has made the application of ultrasound more attractive because of improved image resolution, allowing the analysis of the fine

[*] soz1@psu.edu .

features of tissues. High frequency ultrasound is now widely used in many fields of medical diagnosis, such as dermatologic skin imaging, ophthalmic eye imaging, and catheter-based intravascular (IVUS) imaging.[1, 2]

A piezoelectric transducer is a key component in an ultrasound imaging system, as it acts as both transmitter and receiver and its thickness determines the frequency of vibration. The figure of merit of the piezoelectric element is electromechanical coupling and dielectric permittivity. High coupling piezoelectric materials allow effective energy conversion in both transmitting and receiving energy, improved bandwidth and sensitivity of the transducer response. The dielectric permittivity (ε_r) of piezoelectric material is also an important consideration for the design of a transducer. In order to obtain the maximum transmit and receive sensitivity, the electrical impedance of the transducer should be close to the 50 Ohm imaging electronics.[3] For ultrasound single element and array transducers operating at high frequencies (>20MHz), such as IVUS, very small aperture sizes (<1 mm diameter) are generally used, resulting in mismatched electrical impedance to the imaging electronics. Therefore, it is desirable to use piezoelectric materials with high dielectric permittivity, as well as high electromechanical coupling.

Currently, soft PZT materials, such as PZT-5H, have been the mainstay for low frequency (< 10 MHz) ultrasound transducers due to their high electromechanical properties (k_t~0.50, k_{33} ~0.72)[4]. With reduced grain size, PZT ceramics exhibit higher mechanical strength and better dicing performance, enabling the fabrication of fine pitch and high aspect-ratio piezoelectric elements.[5, 6] Furthermore, in contrast to conventional PZT ceramics, fine-grained PZT ceramics retain their electromechanical properties at high frequencies (>50 MHz), making them suitable for use as high frequency ultrasound transducers.[7, 8]

Recently, relaxor-PT piezoelectric materials, such as $Pb(Mg_{1/3}Nb_{2/3})O_3$-$PbTiO_3$ (PMN-PT), have received attention because they can provide relatively higher dielectric permittivities (ε_r ~6000), nearly twice than that of conventional PZT ceramics, while possessing comparable electromechanical coupling factors (k_{33} ~0.75).[9] Of significant contrast to PZT ceramics, relaxor-PT materials can be grown into large size single crystals, removing scaling limitations associated with high frequency transducers due to grain size issues.

The properties of relaxor-PT single crystals are of great interest for ultrasound transducers, offering exceptional high electromechanical coupling (k_{33}s >0.90),[10, 11] and have now been widely used in commercial ultrasound transducers. In particular, ternary single crystals, $Pb(In_{1/2}Nb_{1/2})O_3$-$Pb(Mg_{1/3}Nb_{2/3})O_3$-$PbTiO_3$ (PIN-PMN-PT), have been found to possess expanded temperature usage range (>120°C) with higher coercive fields (~4-5 kV/cm) than binary PMN-PT crystals, making them more promising candidates for high frequency ultrasound transducers in medical imaging applications.[12, 13]

To date, the size dependent properties of relaxor-PT materials, including polycrystalline ceramics and single crystals, have yet to be investigated. Recent experimental data for PMN-PT crystal/epoxy 1-3 composites operating at frequencies > 40 MHz have revealed a large decrease in electromechanical coupling, leading to the question of the origin of property degradation at high frequency range.[14, 15]

In this work, the electromechanical properties of relaxor-PT materials in polycrystalline and single crystal forms were investigated as a function of scale and corresponding ultrasound frequency to explore degradation mechanisms in relaxor-PT materials.

2. Results & Discussion

2.1 Characterization of Bulk Relaxor-PT Materials

The SEM images of PMN-PT ceramics sintered at 1180°C are shown in Figure 1, compared with the commercial TRSHK1 ceramics (coarse grained PMN-PT). The average grain size of the synthesized PMN-PT was observed to be on the order of 1 micron, whereas the value of commercial TRSHK1 was approximately 7-10 microns.

Electrical properties of relaxor-ferroelectric samples including polycrystalline and single crystal materials were first characterized before investigating the thickness dependent properties. Table I summarizes the room temperature electrical properties of tested relaxor-PT polycrystalline and single crystal materials. The data shown in Table I represents the average of more than 3 samples, and the piezoelectric strain coefficients (d_{33}) were directly determined from a Belincourt meter.

As presented in Table I, the properties of fine and coarse-grained polycrystalline ceramics were similar, with all samples exhibiting high dielectric permittivities being on the order of 6000. For the single crystal forms of PMN-PT, as expected, the piezoelectric and electromechanical properties were superior to those of polycrystalline counterparts. In particular, the longitudinal coupling (k_{33}) was significantly higher than polycrystalline PMN-PTs, being ≥ 90%.

The dielectric and piezoelectric properties of domain engineered ternary PIN-PMN-PT single crystals were comparable to the binary PMN-PT single crystals; moreover, PIN-PMN-PT exhibited two times higher coercive field (E_C) and higher phase transitions temperatures (T_{R-T} & T_C).

2.2. Thickness Dependence Behavior

2.2.1. Dielectric Permittivity—The free and clamped dielectric permittivities of various polycrystalline and single crystal samples, with thicknesses ranging from 500 microns to 30 microns, are plotted in Figure 2. Each value is the average of 3-5 samples, and the error bars represent the standard deviation. The corresponding thickness mode resonance frequencies of the various materials are also added on top of the X-axis of Figure 2, ranging from thickness resonance frequency of 2 MHz to 100 MHz.

For polycrystalline ceramics, the coarse-grained PMN-PT ceramics exhibited a slight decrease in free and clamped dielectric permittivities for samples with thicknesses below 100 microns. Below 50 microns, the strength of coarse-grained samples became problematic; often crumbling apart during polishing, limiting the investigation of frequency less than 40 MHz. However, the fine-grained PMN-PT ceramics allowed the fabrication of much thinner geometries less than 20 microns, corresponding to a resonant frequency of 100 MHz, due to the improved microstructural integrity.

For single crystals, the clamped dielectric permittivity of both PMN-PT and PIN-PMN-PT samples were found to maintain similar values as a function of thickness; however, the free dielectric permittivity of PMN-PT crystals was found to be degraded with decreasing thickness. At a thickness of 40 microns, only half the original value of the free dielectric permittivity was observed for PMN-PT crystals. Of particular significance, the free dielectric permittivity of PIN-PMN-PT samples exhibited minimal thickness dependence, even for the thicknesses less than 50 microns.

2.2.2. Electromechanical Properties—The laterally clamped thickness mode coupling factor (k_t) of relaxor-PT materials were evaluated using the impedance method. Figure 3

shows the measured electrical impedance and phase angle of PMN-PT single crystal samples with different thicknesses. In contrast to free dielectric permittivity of PMN-PT crystals, no degraded k_t (~0.60) was observed in PMN-PT crystals with decreasing thickness, exhibiting a strong and clear resonance and anti-resonance peaks even in the high frequency range (>20 MHz).

The thickness frequency constant (N_t) and k_t of each sample as a function of frequency/sample thickness were summarized in Figure 4. For the coarse-grained PMN-PT ceramics, the k_t was found to exhibit a small decrease with increasing frequency (decreasing thickness), being in the range of 0.45-0.47 at 40 MHz. In contrast, fine-grained PMT-PT ceramics, PMN-PT and PIN-PMN-PT single crystals exhibited stable k_ts in the frequency range studied.

Figure 5 shows the longitudinal electromechanical coupling factors (k_{33}) as a function of frequency for 1-3 composites fabricated by dice-fill technique, and the property change was compared with the values calculated from the permittivities (Figure 2) using equation (1). For comparison, reported experimental data of high frequency (>20 MHz) PMN-PT crystal/epoxy 1-3 composites, fabricated by dry etching method, were also included in Figure 5.

$$k_{33} = \sqrt{1 - \frac{\varepsilon_{33}^{S}}{\varepsilon_{33}^{T}}} \tag{1}$$

From Figure 5, due to their respective thickness dependence of dielectric properties, monolithic fine-grained PMN-PT ceramics and PIN-PMN-PT crystals exhibited original k_{33} values at high frequencies (>20 MHz), while the monolithic PMN-PT crystals exhibited a notable decrease in k_{33} with decreasing thickness and/or increasing frequency. Similarly, PMN-PT 1-3 crystal composites were also found to decrease in couplings (k_{33}) with increasing frequency, while PIN-PMN-PT 1-3 crystal composites were found to maintain higher electromechanical coupling factors at high frequencies (~20 MHz), being on the order of 80%, when compared to PMN-PT 1-3 counterpart, with k_{33} being only ~74% at the same frequency.

2.2.3. Ferroelectric and Piezoelectric Properties—Measurements of polarization versus electric field (P–E) hysteresis loops were performed to examine the influence of the sample thickness on the domain swithcing behavior of each sample. Figure 6 shows P-E hysteresis loops for relaxor-PT ceramics and single crystals with different thicknesses. For PMN-PT single crystals, the clamping/pinning of domain wall motion is evident, exhibiting a noticeable change in coercive field, E_C and remnant polarization, P_r with decreasing thickness. The P_r and E_C of thick PMN-PT crystals (500 microns) were initially 27 $\mu C/cm^2$ and 2.5 kV/cm, respectively, changing to 20 $\mu C/cm^2$ and 3.5 kV/cm when the thickness reduced to 50 microns. In contrast, fine-grained PMN-PT ceramics and ternary PIN-PMN-PT single crystals maintained original values of P_r and E_C with decreasing thicknesses, indicating no clamping/pinning of domain wall motion even at the thicknesses of 50 microns.

The high-field piezoelectric behavior for the polycrystalline and single crystals with different thicknesses are given in Figure 7 and 8, respectively. For coarse-grained PMN-PT ceramics, the high-field piezoelectric coefficients (d_{33}) calculated from strain-field curves maintained similar values with decreasing thicknesses down to 100 micron. Then, a decrease in maximum strain level was observed when the sample thicknesses were less than 100 microns. At a thickness of 50 micron, the high-field d_{33} was found to be 650 pm/V. For fine-grained PMN-PT ceramics, on the other hand, the unipolar strain levels were found to

maintain the same values, being on the order of 900 pm/V, with decreasing thicknesses down to 30 microns.

For PMN-PT single crystals, the high field d_{33}s were found to degrade significantly, with the values being on the order of 1800 pm/V and 1000 pm/V for 500 micron and 40 micron samples, respectively. In contrast, ternary PIN-PMN-PT single crystals maintained original strain levels down to 40 micron thicknesses. However, it should be noted that all samples exhibited increased strain hysteresis at small thicknesses, implying domain instability with decreasing thickness.

2.3. Discussion

2.3.1. Surface Damage (Low Polarizable Surface Layer)—Degraded dielectric and piezoelectric properties with decreasing thickness can often be related to surface damage (low polarizable surface layer) as a result of lapping and/or polishing. Experimental evidence that the properties of damaged surfaces are different from those of bulk specimens has been previously reported. Subbarao et al.[16] measured surface polarization using thermal and acoustic pulse measurements, revealing a decrease in polarization in the regions closest to the surface compared to the overall polarization. Jyomura et al.[17] studied the influence of lapped surfaces on the dielectric properties, and found that the samples prepared by lapping exhibited a lower dielectric permittivity and remnant polarization, compared to the samples prepared by chemical etching. Furthermore, using X-ray diffraction, Cheng et al.[18] and Mehta et al.[19] observed domain reorientation in surface regions well beyond that achieved by the electric field when the sample surfaces were finished with grinding and/or polishing by 45 micron diamond. The results indicate that low polarizable surface layers can be formed as a result from surface-finishing stresses and/or damage.

In order to examine the presence of surface damage on the samples in this study, X-ray analysis was carried out. Since the penetration depth of X-ray is on the order of a few microns, X-ray can examine surface damage.[20, 21] Figure 9 shows an X-ray profile of a fine-grained PMN-PT polycrystalline ceramic prepared by final surface finishing with 0.05 micron particles. For comparison, Figure 9 also includes an X-ray profile of the same ceramic prepared by dicing, which is known to generate surface damage.[22, 23] Note that the X-ray profile of coarse-grained PMN-PT is not included here due to the same X-ray behavior as observed for fine-grained PMN-PT.

For the sample prepared by polishing, a noticeable change in the intensity ratio of (200) and (002) X-ray reflections was observed after poling. In contrast, diced samples did not exhibit the change in intensity ratio after poling. This demonstrate that mechanical dicing led to the rotation of non-180 degree domains and the formation of 180 degree domains in the surface regions prior to poling, hindering the surface polarization upon poling.[18]

Figure 10 demonstrates the XRD profiles taken from the polished surface of PMN-PT and PIN-PMN-PT single crystals. For comparison, the diced surfaces were also X-rayed and included in Figure 10. Note that the peak splitting observed in PMN-PT crystals was due to Cu $K\alpha_2$ contribution. As shown, the XRD profiles of diced surfaces of both samples exhibited broad peaks in the 2θ angles from 20 to 120°, compared to those of polished surfaces, indicating the presence of surface damage caused by dicing stress.

From the above results, the degraded electrical properties observed in relaxor-PT materials could be, to some extent, attributed to surface damage, especially when the sample thickness approaches to the dimension of surface damage layer. As observed in Figure 5, the level of decrease in coupling of PMN-PT 1-3 crystal composites fabricated by dry etching technique was less severe, when compared to the 1-3 composites fabricated by dice-fill technique.

However, the monolithic samples in this study were prepared by polishing with very fine particles (0.05 micron) and post-annealing, which can minimize or eliminate the surface damage on samples. Therefore, it can not be explained that the surface damage is a primary origin for degraded properties of monolithic PMN-PT crystals with decreasing thickness.

2.3.2. Ferroelectric Domains—A reduction in dielectric and piezoelectric properties may also be associated with the ferroelectric domains. The fact that the origin of a large dielectric and piezoelectric response of <001> poled relaxor-PT single crystals is closely related to the domain engineered 4R structures and polarization rotation mechanism.[25-27] On the microscopic scale, poling along <001> in rhombohedral relaxor-PT crystals creates four degenerate domain variants, and the dipoles in domains can be aligned along any one of the four equivalent <111> directions.

When the sample dimension is much larger than domain size, four types of domains will be equally populated and formed stable multidomain (4R) configuration, the large shear mode properties, corresponding to an easy polarization rotation, will contribute to the large dielectric permittivity K_{33}^{T} and piezoelectric d_{33} in relaxor-PT crystals. However, when the physical size of the samples becomes of the same order as the domain size, it is possible that the surface boundary condition may disrupt the equilibrium 4R domain structures and impede tendency for a polarization rotation. This might explain an increase in strain hysteresis of relaxor-PT crystals at small thicknesses, as seen from Figure 8, since anhysteretic strain-field behavior of <001>-poled relaxor-PT crystals is the consequence of stable 4R domain structures.

In order to delineate the influence of ferroelectric domains on the observed degraded properties, the dielectric permittivity of PMN-PT single crystals with different thicknesses were investigated as a function of temperature. If the ferroelectric domain is a primary origin for degraded properties, it can be expected that the permittivities of thin PMN-PT crystals in the paraelectric state (above T_C) exhibit similar values as those of normal size PMN-PT crystals, where no domains exist.

The dielectric permittivity and loss as a function of temperature for PMN-PT and PIN-PMN-PT crystals are presented in Figure 11 for different thicknesses. In the temperature range below T_{R-T} (the rhombohedral to tetragonal phase transition temperature), the dielectric permittivity for PIN-PMN-PT crystals was found to exhibit nearly thickness independent dielectric behavior, while for PMN-PT crystals, the permittivity of the 50 micron-sample was found to be much lower than that of thick samples.

However, in the region between T_{R-T} and T_C, where the crystals are in the temperature induced tetragonal phase region, the thickness dependent behavior was found to be opposite to those of rhombohedral crystals, exhibiting that both 50 micron PMN-PT and PIN-PMN-PT crystals showed higher permittivities compared to 500 micron thick samples, indicating that the single domain state in tetragonal phase became unstable at small thicknesses.[24]

As the temperature approached to T_C, the dielectric permittivity of 50 micron PMN-PT samples exhibited broader peaks as well as depression of dielectric maxima compared to thick PMN-PT samples, while 50 micron PIN-PMN-PT samples exhibited comparable dielectric maxima to 500 micron PIN-PMN-PT samples, demonstrating severe surface boundary/domain effects in thin PMN-PT samples.

For temperatures well beyond T_C, where no domains exist, both thin and thick samples exhibited same values and showed same trend as a function of temperature, which in reverse, indicates that the degraded properties of PMN-PT single crystals at room

temperature are closely associated with the domain effects. The same phenomena were also observed in PMN-PT polycrystalline ceramics, where the dielectric permittivities exhibited thickness independent behavior when temperature above T_C.

From the temperature dependence of the dielectric properties, it appears that the observed different thickness dependence of the dielectric and piezoelectric properties of relaxor-PT materials are related to an increased surface boundary effect with decreasing thickness, as a result from their respective domain sizes.

For polycrystalline ceramics, it has been reported that the domain size of ferroelectric ceramics is proportional to the square root of the grain size,[28, 29] implying that the domain sizes of fine-grained PMN-PT are smaller than those of coarse-grained PMN-PT. As expected, the fine grained PMN-PT ceramics were found to possess minimal thickness dependent properties when compared to their coarse-grained counterparts.

For single crystals, the domain sizes of PMN-PT crystals are much larger than those of polycrystalline ceramics, with sizes being on the order of 10-100 microns.[21] Consequently, due to the comparable sample sizes to the domain sizes of PMN-PT crystals, both “extrinsic”, i.e., contribution of the irreversible domain wall motion, and “intrinsic” from polarization rotation, can be suppressed by surface boundary conditions when the sample thickness is on the order of domain size. For the case of PIN-PMN-PT crystals, however, since no degraded dielectric permittivity was observed in the thickness range from 500 to 40 microns, it can be expected that ternary PIN-PMN-PT crystals possess smaller domain size compared to binary PMN-PT crystals.

Figure 12 shows the optical micrographs of poled PMN-PT and PIN-PMN-PT single crystals taken through crossed polarizers. It is evident from these figures that the domain sizes of poled PIN-PMN-PT crystals are much smaller, being on the order of 1 micron, compared to those of poled PMN-PT crystals, being on the order of 10-20 micron. These observations confirm that the domain sizes are responsible for thickness dependence of dielectric and piezoelectric properties.

3. Conclusions

To enhance the applicability of relaxor-PT polycrystalline ceramics for high frequency transducer materials, fine-grained (<1micron) PMN-PT ceramics were fabricated, and the properties were compared with those of commercial PMN-PT ceramics (TRSHK1), whose grain size is around 7-10 micron (coarse-grained PMNT). Compared to coarse-grained materials (TRSHK1), fine-grained PMN-PT ceramics allowed the fabrication of high frequency (>40 MHz) ultrasound transducers without breakage.

For single crystals, it was found that domain size plays a dominant role in property degradation with decreasing thickness. Degradation in permittivity was observed in PMN-PT crystals with decreasing thicknesses due to the increased surface boundary effects. In contrast to PMN-PT crystals, PIN-PMN-PT exhibited excellent property stability at high frequencies (>50MHz), with minimal thickness dependence down to 40 microns, due to their relatively smaller domain sizes. The results suggest that fine-grained PMN-PT ceramics and ternary PIN-PMN-PT single crystals are promising candidates for high frequency ultrasound transducer applications.

4. Experimental

Materials

Commercially available TRSHK1, [modified PMN-PT with composition near the morphotropic phase boundary (MPB)] polycrystalline ceramics were obtained from TRS technologies Inc. Relaxor-PT single crystals, including PMN-PT and PIN-PMN-PT, were grown using the modified Bridgman method. Rhombohedral compositions away from the MPB were selected to avoid the phase variation effect on the properties.

Fine-grained (≤1 micron) PMN-PT ceramics were fabricated using PMN-PT powder (same composition as TRSHK1) from TRS technologies Inc., to eliminate the possible influence of dopant or composition effects. Sub-micron particles were prepared from attrition milling for 8 hours. A commercial dispersant, Darvan 821A (R.T.Vanderbilt Company Inc., CT) with ammonium hydroxide solutions (NH_4OH) were used for the preparation of the well-dispersed slurry. To minimize contamination, high purity and high strength zirconia media balls were used during the milling process. Binder was added to the milled powder and granulated to maintain strength for pressing. The granulated powders were pressed into pellets of 20 mm in diameter and 2-3 mm thickness, and sintered at 1180 °C. After sintering, the pellets were hot isostatically pressed (H.I.P) at 1080 °C for 2 hours in an O_2/Ar atmosphere to eliminate residual porosity.

Samples Preparation

Samples of both polycrystalline and single crystal materials with various thicknesses were prepared by lapping and polishing. Initial lapping utilized 15 micron Al_2O_3 powder suspended in a distilled water medium. Final lapping was carried out with a 0.05 micron diamond paste to minimize surface damage which can deteriorate the material properties. Gold sputtering was used to deposit electrodes on both surfaces. The samples were then drilled or cut to the desired dimensions with diameter to thickness ratios of ≥20. This ensured that any lateral mode harmonics would not interfere with the fundamental thickness mode. All samples were then annealed at 400°C for 5 hours in order to alleviate residual stress.

For the fabrication of 1-3 composites, the samples were diced using an automatic dicing machine, K&S 982-6 (Kulicke & Soffa Industries, Willow Grove, PA). The samples were first diced along one direction with a spindle speed of 30,000 rpm and a feed rate of 1.5 mm/sec, then diced in the perpendicular direction. A low viscosity epoxy (Epotek 301, Bellerica, MA) was then backfilled into the kerfs in vacuum for 30 minutes, and subsequently cured at room temperature for 24 hours. The fabricated composites were polished until all the piezoelectric posts were exposed, and gold electrodes were sputtered on both surfaces.

All the samples were then poled at room temperature at an electric field two times their respective coercive fields (E_C).

Physical Properties Measurements

The grain size of the polycrystalline ceramics were analyzed by means of a scanning electron microscope (SEM, S-3500N, Hitachi, Tokyo, Japan). The domain structure of poled single crystals were examined using a polarizing light microscope (Olympus BX60) in transmission mode. For domain observations, the samples were prepared by polishing to the thicknesses of 50-100 microns using diamond paste (1 micron).

X-ray analysis was carried out using an X-ray diffractometer (PANalytical) with Cu Kα radiation equipped with XPert Pro MPD with the operation voltage and current of 40kV and 40 mA, respectively.

Electrical Properties Measurements

The free (K_{33}^T) and clamped (K_{33}^S) dielectric permittivity and coupling factors (k_t and k_{33}) of the prepared samples were determined using a multi-frequency LCR meter (HP4284A) and an HP4194A impedance- phase gain analyzer, respectively. The free and clamped dielectric permittivities were calculated from the capacitance measurements according to the following equation (2).

$$K_{33}=\frac{C\cdot t}{A\cdot \varepsilon_0} \tag{2}$$

where ε_0 is free space dielectric permittivity, A is the area of the sample, t is the thickness, C is the capacitance measured at 1kHz frequency for free permittivity and at the frequency of 2 f_a for the clamped permittivity. The dielectric behavior as a function of temperature was determined using a multi-frequency HP4284A LCR meter connected to a computer-controlled furnace.

The thickness mode electromechanical coupling factor (k_t) and frequency constant (N_t) were determined using the following equations (3) and (4), respectively.

$$k_t^2=\frac{\pi}{2}\frac{f_r}{f_a}\cot\left(\frac{\pi}{2}\frac{f_r}{f_a}\right) \tag{3}$$

$$N_t=f_r\times t \tag{4}$$

where f_r and f_a are the thickness resonance and anti-resonance frequencies, respectively, and t is the sample thickness.

Polarization versus electric field (P-E) and unipolar strain were measured at 1 Hz frequency using a modified Sawyer-Tower circuit and linear variable differential transducer (LVDT) driven by a lock-in amplifier (Stanford Research Systems, Model SR830). The remnant polarization, P_r and coercive field, E_C were determined from the hysteresis loops at a driving field of 20 kV/cm.

The high field piezoelectric coefficients (d_{33}) were determined from the slope of strain / field curves at the driving field of 10 kV/cm. Strain hysteresis was calculated from equation:

$$\text{Strain hysteresis}\,(\%)=\frac{\Delta x}{x_{max}}\times 100 \tag{5}$$

where x_{max} is the maximum strain and Δx is the strain deviation during the rise and fall of the field at half of the maximum electric field.

Acknowledgments

This work supported by the NIH under Grant No. P41-EB21820 and ONRunder Grant Nos. N00014-09-1-01456, N-00014-07-C-0858.

References

[1]. Lockwood G, Turnball D, Christopher D, Foster F. IEEE Eng. Med. Biol. Mag. 1996; 15(6):60–71.

[2]. Pavlin CJ, Simpson ER, Foster FS. Ultrasound Clinics. 2008; 3:185–194.

[3]. Smith WA. Proc. SPIE. 1992; 1733:3–26.

[4]. Shung KK, Cannata JM, Zhou QF. J. Electroceram. 2007; 19:139–145.

[5]. Hackenberger W, Pan M-J, Vedula V, Pertsch P, Cao W-W, Randall C, Shrout T. Proc. SPIE. 1998; 3324:28–36.

[6]. Hackenberger W, Rehrig PW, Ritter T, Shrout T. Ultrason. Symp. IEEE. 2001; 2:1101–1104.

[7]. Foster F, Ryan L, Turnbull D. IEEE Trans. Ultrason., Ferroelect., Freq. Contr. 1991; 38:446–453.

[8]. Zipparo MJ, Shung KK, Shrout TR. IEEE Trans. Ultrason., Ferroelect., Freq. Contr. 1997; 44:1038–1048.

[9]. Wang H, Jiang B, Shrout T, Cao W. IEEE Trans. Ultrason., Ferroelect., Freq. Contr. 2004; 51:908–912.

[10]. Kuwata J, Uchino K, Nomura S. Jpn. J. Appl. Phys. 1982; 21:1298–1302.

[11]. Park SE, Shrout TR. J. Appl. Phys. 1997; 82:1804–1811.

[12]. Tian J, Han P, Huang X, Pan H, Carroll JF Iii. Appl. Phys. Lett. 2007; 91:222903.

[13]. Zhang S, Luo J, Hackenberger W, Shrout T. J. Appl. Phys. 2008; 104:064106.

[14]. Jiang X, Snook K, Hackenberger W, Cheng A, Xu J. IEEE Sensors. 2008:573–576.

[15]. Jiang X, Snook K, Walker T, Portune A, Haber R, Geng X, Welter J, Hackenberger W. Proc. SPIE. 2008; 6934:69340D.

[16]. Subbarao EC, McQuarrie MC, Buessem WR. J. Appl. Phys. 1957; 28:1194–1199.

[17]. Jyomura S, Matsuyama I, Toda G. J. Appl. Phys. 1980; 51:5838–5844.

[18]. Cheng S, Lloyd IK, Kahn M. J. Am. Ceram. Soc. 1992; 75:2293–2296.

[19]. Mehta K, Virkar A. J. Am. Ceram. Soc. 1990; 73:567–574.

[20]. Durbin MK, Jacobs EW, Hicks JC, Park SE. Appl. Phys. Lett. 1999; 74:2848–2850.

[21]. Lim L, Kumar F, Amin A. J. Appl. Phys. 2003; 93:3671–3673.

[22]. Goat CA, Whatmore RW. J. Eur. Ceram. Soc. 1999; 19:1311–1313.

[23]. Nix E, Corbett J, Sweet J, Ponting M. CARTS Europe. 2005; 19:246–258.

[24]. Zhang S, Luo J, Xia R, Rehrig P, Randall C, Shrout T. Solid State Commun. 2006; 137:16–20.

[25]. Damjanovic D. IEEE Trans. Ultrason., Ferroelect., Freq. Contr. 2009; 56:1574–1585.

[26]. Fu H, Cohen R. Nature(London). 2000; 403:281–283. [PubMed: 10659840]

[27]. Davis M, Budimir M, Damjanovic D, Setter N. J. Appl. Phys. 2007; 101:054112.

[28]. Arlt G, Hennings D, de With G. J. Appl. Phys. 1985; 58:1619–1625.

[29]. Cao W, Randall C. J. Phys. Chem. Solids. 1996; 57:1499–1505.

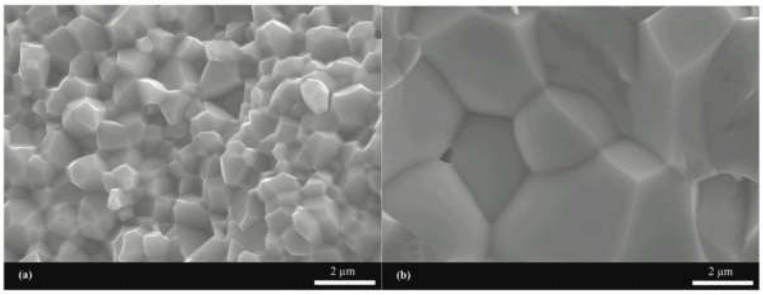

Figure 1.
SEM images of the microstructure of fine (a) and coarse (b) grained PMN-PT ceramics.

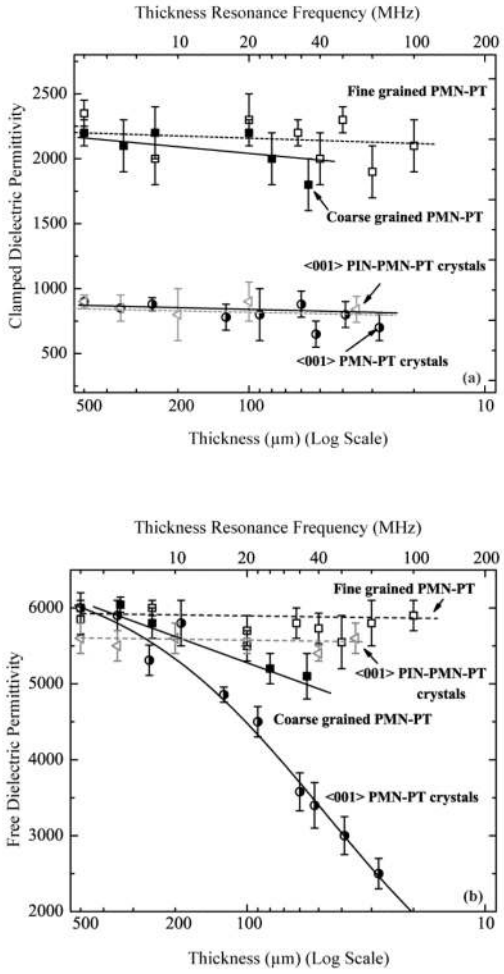

Figure 2.
Clamped (a) and free (b) dielectric permittivities of relaxor-PT materials as a function of thickness and corresponding ultrasound frequency.

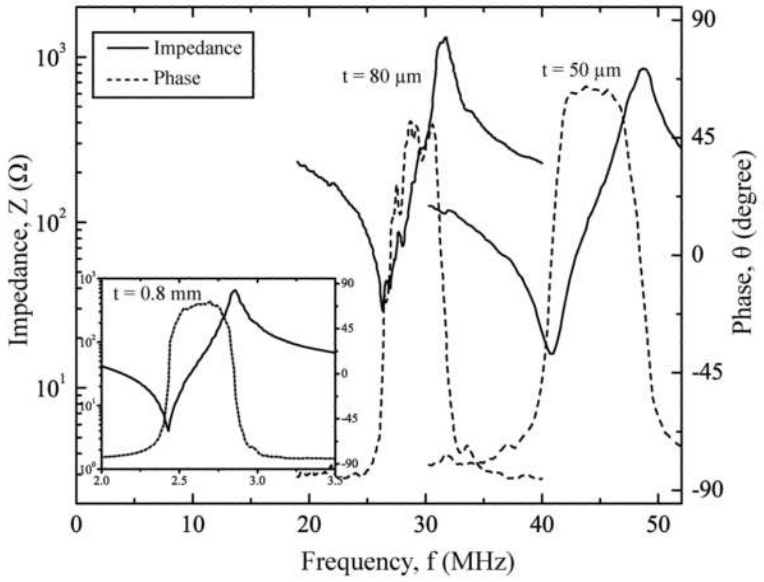

Figure 3.
Measured electrical impedance (solid line) and phase (dashed line) of <001>-poled PMN-PT single crystals with different thickness (t).

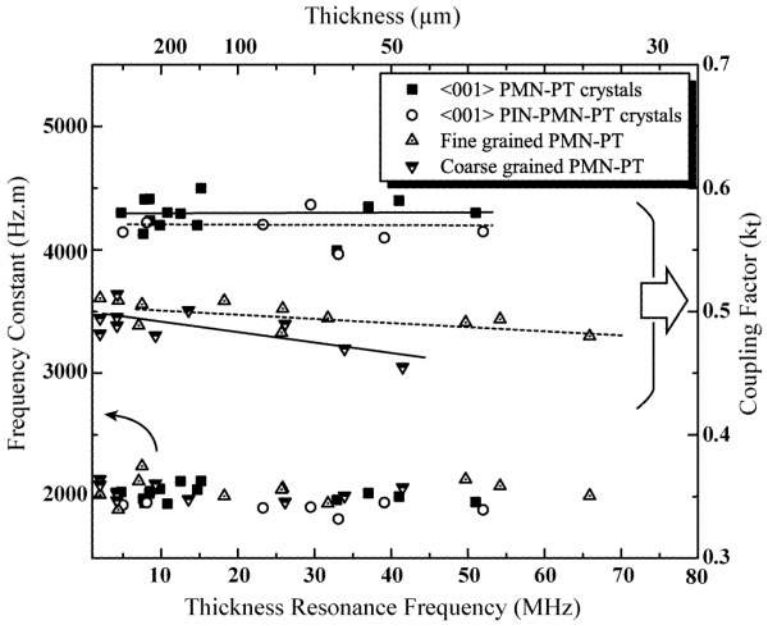

Figure 4.

Thickness/frequency dependence of frequency constant (N_t) and thickness mode electromechanical coupling factor (k_t) for relaxor-PT materials.

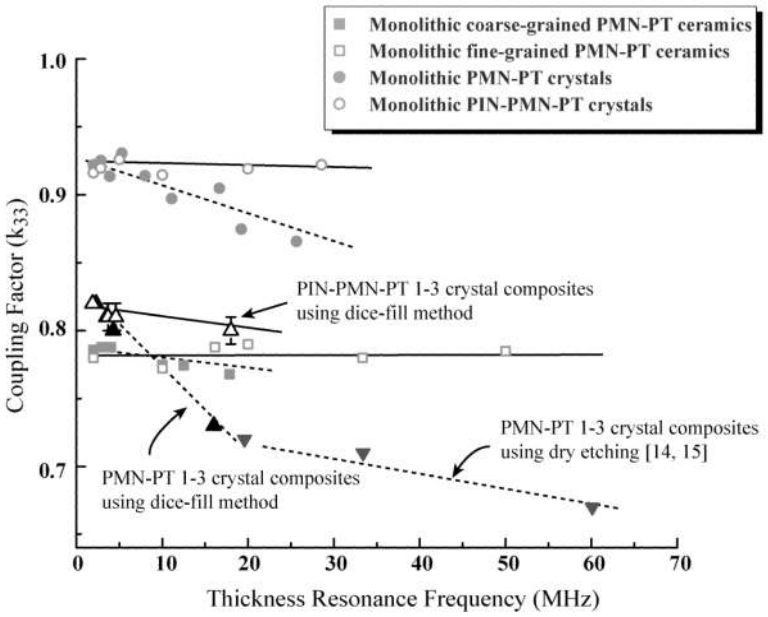

Figure 5.

Frequency dependence of electromechanical coupling factors (k_{33}) for relaxor-PT materials. Data for PMN-PT/epoxy composites fabricated by dry etching (PC-MUT) are obtained from Refs [14, 15].

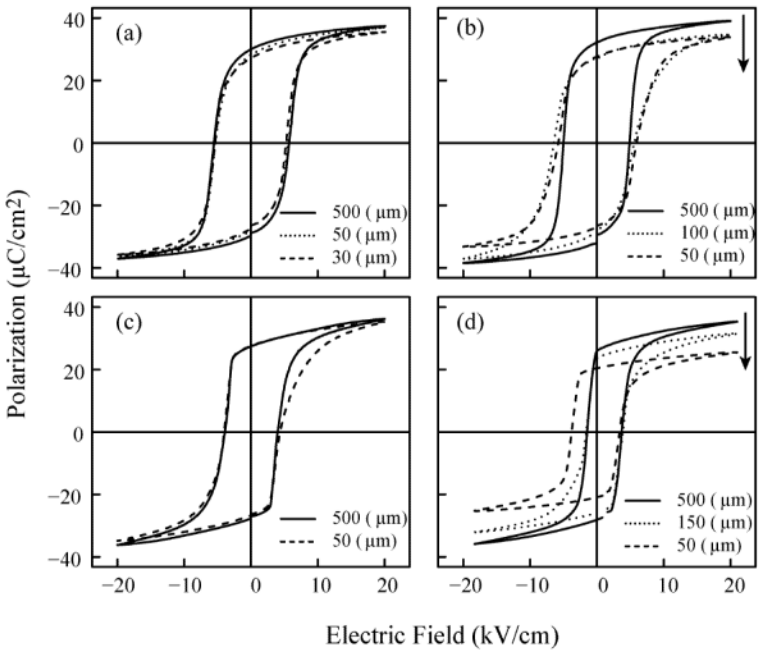

Figure 6.
Polarization hysteresis as a function of electric field for relaxor-PT materials as a function of thickness. (a) fine grained PMN-PT (b) coarse grained PMN-PT (c) PIN-PMN-PT crystals (d) PMN-PT crystals. Arrow indicates decreasing thickness.

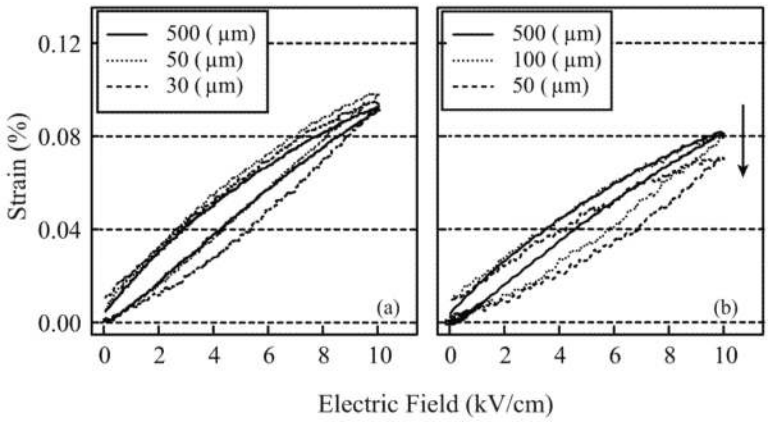

Figure 7.
Thickness dependence of unipolar strain as a function of electric field for (a) fine-grained and (b) coarse-grained PMN-PT ceramics. Arrow indicates decreasing thickness.

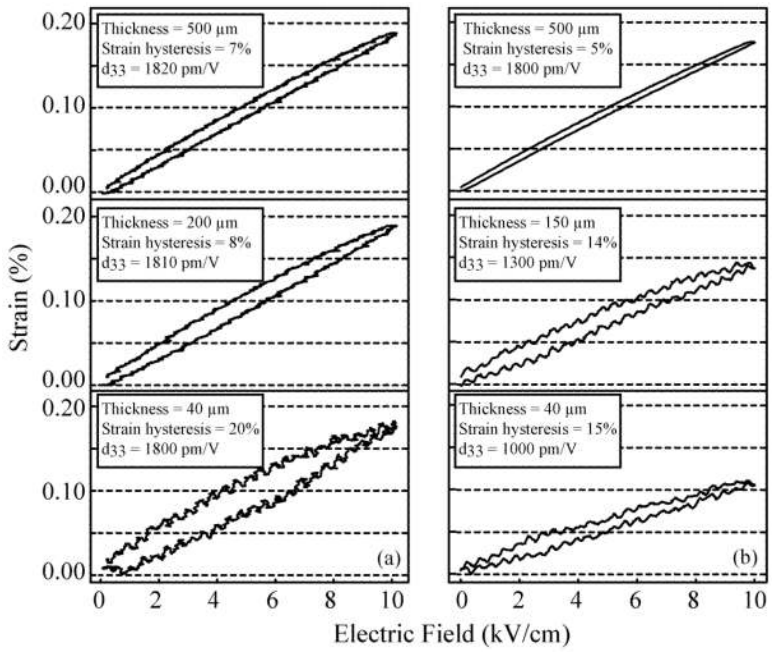

Figure 8.

Thickness dependence of unipolar strain as a function of electric field for <001>-poled (a) PIN-PMN-PT and (b) PMN-PT crystals.

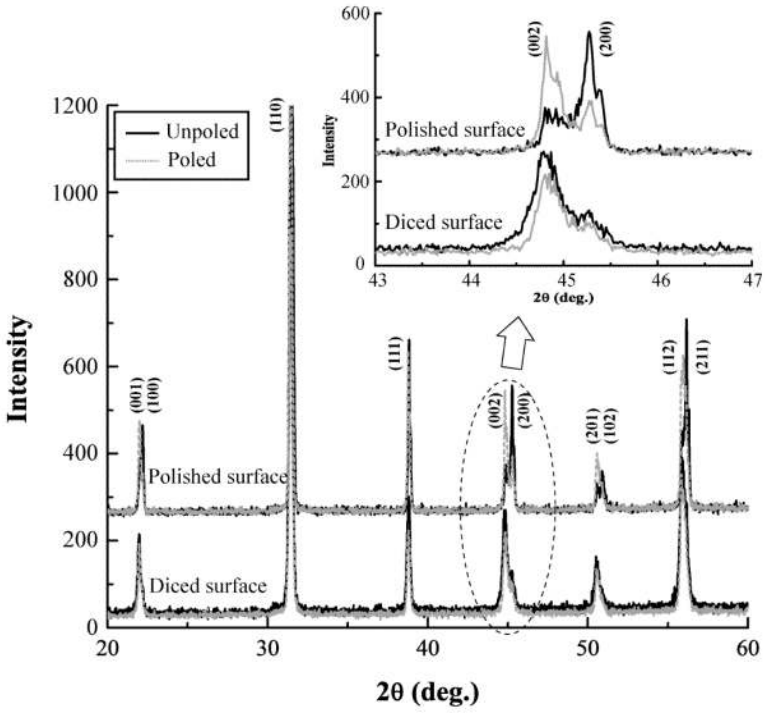

Figure 9.
X-ray diffraction patterns on the surfaces of fine-grained PMN-PT ceramics (Inset shows enlarged X-ray patterns with 2θ in the range of 43-47°).

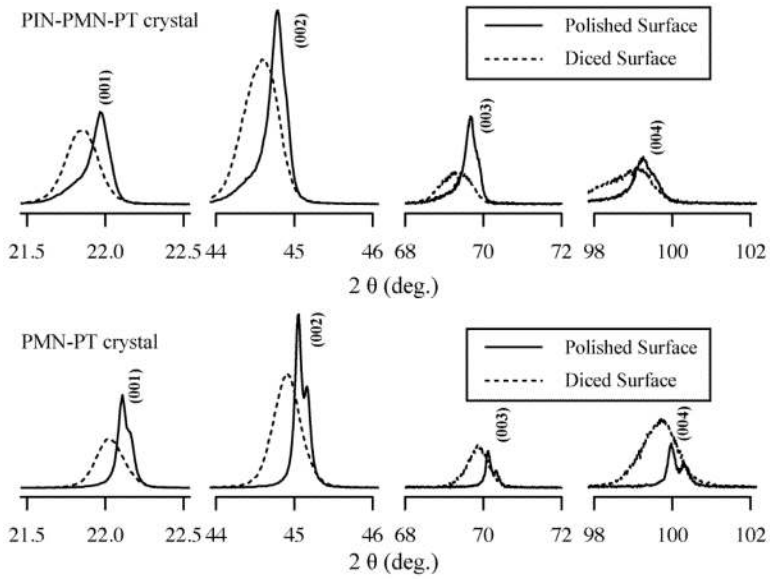

Figure 10.
X-ray diffraction patterns on the surfaces of relaxor-PT single crystals.

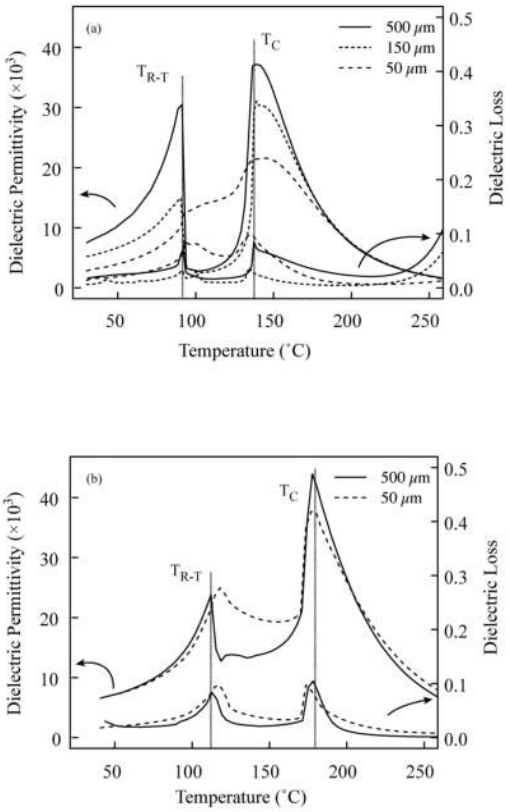

Figure 11.
Dielectric permittivity and loss as a function of temperature for <001>-poled PMN-PT (a) and PIN-PMN-PT (b) single crystals with different thickness.

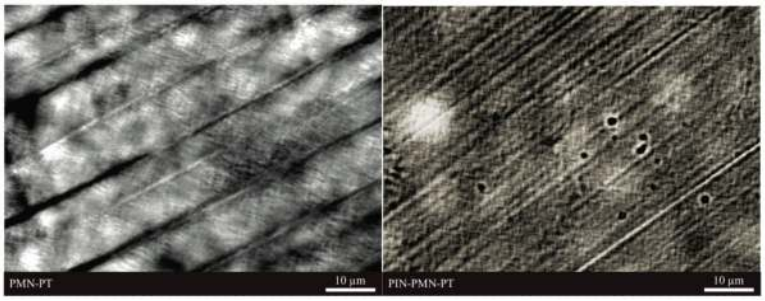

Figure 12.
Domain configurations of PMN-PT (a) and PIN-PMN-PT (b) single crystals using polarized optical microscopes.

Table I

Characterization of bulk relaxor-PT ceramics and crystals. (Thickness >500 μm)

Parameter	**Fine Grain PMN-PT**	**TRSHK1**	**PMN-PT**	**PIN-PMN-PT**
Form	Polycrystalline Ceramic	Polycrystalline Ceramic	Single Crystal	Single Crystal
Grain Size (μm)	<1	7-10	-	-
T_C (°C)	150	150	135	178
T_{R-T} (°C)	-	-	95	113
Orientation	-	-	001	001
Free permittivity	5900	6000	6000	5600
Clamped permittivity	2500	2200	900	900
Dielectric loss	0.025	0.016	0.004	0.006
d_{33} (pC/N)	820	850	1800-2000	1900
P_r (μC/cm^2)	30	32	27	27
E_c (kV/cm)	5.5	5.0	2.5	5.0
k_t	0.50	0.51	0.60	0.56
k_{33}	0.73	0.74	0.90	0.91